ChemComm

Accepted Manuscript

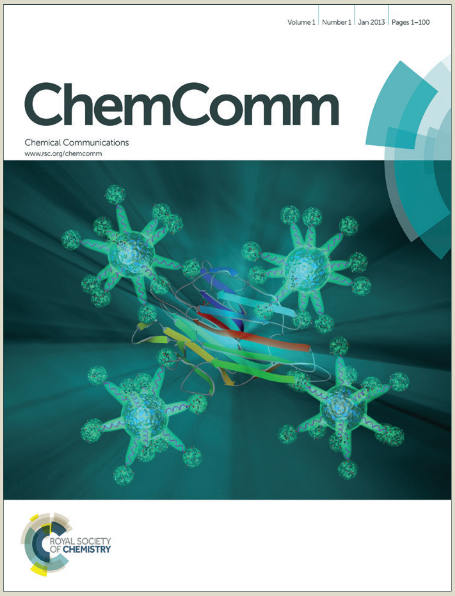

ROYAL SOCIETY
OF **CHEMISTRY**

www.rsc.org/chemcomm

ChemComm RSCPublishing

COMMUNICATION

Organic-free synthesis of ultrathin gold nanowires as effective SERS substrates

Cite this: DOI: 10.1039/x0xx00000x

Received 00th January 2015,
Accepted 00th January 2015

DOI: 10.1039/x0xx00000x

www.rsc.org/

Man Zhou,[a] Ming Lin,[b] Yongzheng Wang,[a] Xuefeng Guo,*[a] Xiangke Guo,[a] Luming Peng,[a] and Weiping Ding[a]

We present a novel and facile fabrication of ultrathin gold nanowires in the absence of organic reagent. Measurements of surface-enhanced Raman scattering (SERS) demonstrated that the obtained organic-free ultrathin Au nanowires can serve as simple and effective SERS substrates.

One-dimensional (1D) metal nanostructures (*i.e.* nanorods, nanobelts, nanotubes, nanowires) have attracted increasing attentions because of their unique physical and chemical properties.[1,2] Among these 1D nanomaterials, gold nanowires (Au NWs) with high aspect ratios, are of particular interest owing to their excellent electrical, optical and chemical properties.[3-5] As a result, the applications of gold nanowires cover many fields including but not limited to highly sensitive biosensor,[6] gas sensors,[7] highly active catalysts,[8] mechanical energy storage and release,[9] flexible electrodes with high transparency and conductivity,[10] surface-enhanced Raman scattering (SERS),[11,12] *etc*. Obviously, preparation of organic-free Au NWs is one of the basic requirements for all these applications.

In the past decade, great efforts have been devoted to the synthesis of Au NWs, especially the ultrathin Au NWs (diameter < 2 nm). In 2007, Halder and Ravishankar demonstrated a multi-step strategy of obtaining ultrathin Au NWs in toluene using a mixture of oleic acid, oleylamine (OA) and ascorbic acid.[13] Since then, several important progresses have been made by different groups for the synthesis based on this wet-chemical method. For example, Xia *et al*. improved this method by slowly reducing the polymeric strands of OA-AuCl complexes which was described as a linear chain composed of a $Au^I \cdots Au^I$ backbone.[14] Yang *et al*. reported the mesostructures consisting of $HAuCl_4$ and OA which served as growth template during the synthesis.[15] In 2012, Zhang *et al*.[16] and Ravishankar *et al*.[17] extended this OA system to various substrates such as graphene oxide, Cu grid, SiO_2/Si and Si_3N_4. Besides OA, some derived organics, *e.g.* poly(amidoamine)[18] and long-chain amidoamine,[19,20] could also acted as stabilizing agents for the synthesis of ultrathin Au NWs. In general, OA is the most efficient reducing agent and soft template to direct Au nanowire growth.[21-23] However, all above organic compounds with long chain aliphatic amine were hard to be removed, which overshadowed the further investigates and application.[24] So far, the fabrication of ultrathin Au NWs in the absence of organic reagent still remains a great challenge.

In this communication, we present a novel and organic-free route for the synthesis of ultrathin Au NWs at room temperature within a few hours. Only three inorganic materials ($HAuCl_4$, Cu sheets and carbon-coated Cu grid) were involved throughout the entire synthetic procedure. Cu sheets acted as pre-reducing agent and carbon-coated Cu grid as substrate for one-dimensional growth. The obtained surface-clean Au nanowires on Cu grid could be directly used as an active substrate for surface-enhanced Raman scattering (SERS) application.

In a typical synthesis, as illustrated in Fig. 1, Cu sheet with thickness of ~ 0.6 mm was cut into two pieces with rectangular shape (0.5 cm × 3 cm). The copper sheets were firstly placed into 2 mL $HAuCl_4$ aqueous solution (0.1 M). Meanwhile, the whole reaction system was kept still under ultrasonic treatment for about 30 seconds. Then, the light green colloid suspension was collected after removing large particles by low-speed centrifugation (2000 rpm, 5 min). Afterwards, a fresh carbon-coated Cu grid was positioned on medium speed filter papers tilted 30° from the horizontal plane. A few droplets of the seed solution were carefully dropped onto the carbon-coated Cu grid. Finally, after being washed with water for several times and natural drying process at room temperature, ultrathin Au NWs with clean surfaces were obtained on Cu grid substrate.

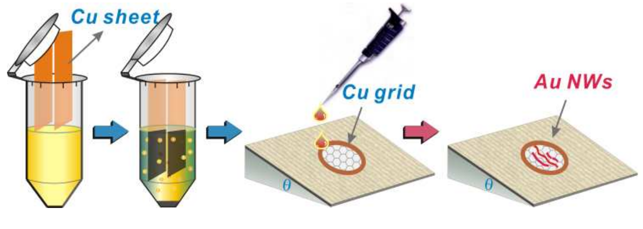

Fig. 1 Illustration of synthetic process of ultrathin Au NWs. θ is the oblique angle between Cu grid and the horizontal plane.

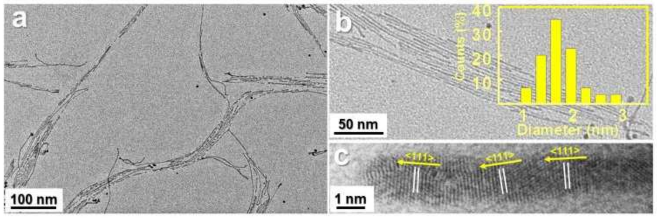

Fig. 2 (a-b) TEM image of ultrathin Au NWs obtained on Cu grid. Inset: diameter distribution histogram of ultrathin Au NWs calculated from HRTEM images. (c) High-resolution TEM image of a single Au NWs.

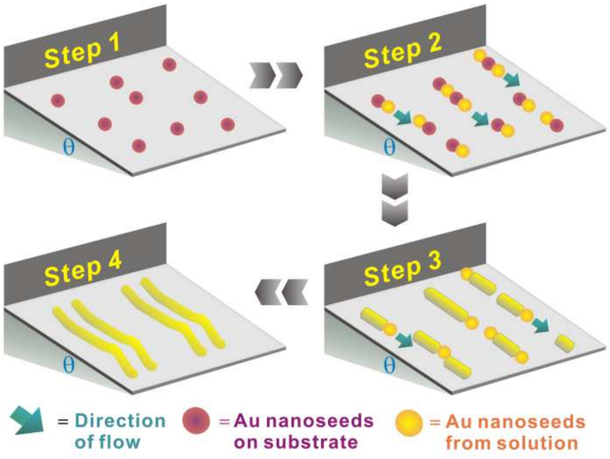

Fig. 4 Possible mechanism for the growth of ultrathin Au NWs on Cu grid.

Transmission electron microscopy (TEM) images were directly obtained on Cu grid substrate. The product mainly consists of ultrathin Au nanowires with an average diameter of 1.8 ± 0.4 nm and length up to micrometers (see Fig. 2a-2b). These TEM images suggested the good continuity of the ultrathin Au NWs. The composition of the nanowires is also confirmed by EDX analysis (see Fig. S1, ESI†). The spectrum shows exclusively Au peaks apart from Cu signals. According to high-resolution TEM results, both single-crystalline and polycrystalline wires with stacking faults were formed after reaction (see Fig. 2c). The spacing of observed lattice fringes is 0.23 nm, corresponding to the distance between {111} crystal planes. By measuring the angle between {111} planes and growth direction of nanowires, it was found that most of the single crystalline wires were grown along <111> direction, while the remaining along <100> direction, which suggested by an angle of ~56° between {111} and {100} planes (see Fig. S2, ESI†). Fig. 2c demonstrate a typical polycrystalline wires grown along <111> direction, the slight deviation of the {111} planes in each grain indicated that the wire could be formed *via* an oriented attachment process.[25] Similar phenomena have been reported by Liu *et al*.[18]

In order to investigate the morphology changes during the whole procedure, drops of seed solution were controlled to give a comparison. As shown in Fig. 3a, only small Au nanoparticles (Au NPs) were observed after adding the first drop of the seed solution. With two drops of seed solution (see Fig. 3b), Au nanorods (Au NRs) or short Au NWs were formed besides small Au NPs. After adding the third drop (see Fig. 3c), although few Au NPs could also been found, Au NWs with uniform morphology were formed with a diameter of ~1.8 nm and length up to ~50 nm. More details can be checked in Fig. S3, ESI†. Furthermore, upon adding the fourth drop (see Fig. 3d), Au NWs rapidly grew up to ~ 500 nm on the substrate while the amount of nanoparticles was significantly reduced.

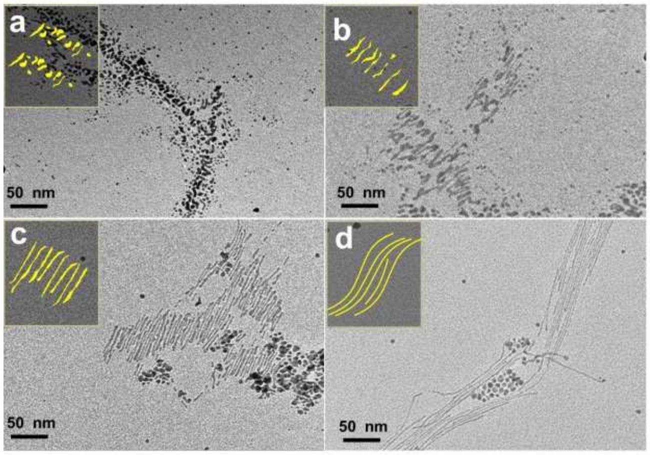

Fig. 3 TEM images of Au nanostructures obtained at different stages of adding the seed solution onto the Cu grid. (a) one, (b) two, (c) three and (d) four drops.

The Au nanowires display long-term stability on the Cu grid which exhibits no noticeable changes in TEM images after being placed for a week (see Fig. S4, ESI†). However, during lengthy TEM examinations we easily observed morphological changes upon exposure to high-energy beams. The structure of ultrathin Au NWs was quickly damaged by incident high-energy electron beam, and prolonged exposure resulted in fractures and conversion into particles from fragments (see Fig. S5, ESI†). This morphological change could be triggered by two reasons, the high localized temperature heated by electron beams and the surface diffusion of Au atoms on clean and unprotected wire surface without conventional surfactant.

On the basis of the above results, a growth mechanism for the ultrathin Au NWs was proposed in Fig. 4. Firstly (at the first drop of the seed solution), most of reduced Au nanoseeds (Au NSs) were separated to each other after being located on the carbon membrane (as shown in step 1). Then, as continual dropping colloidal solution containing ultra-small Au NSs as well as Au^+ ions on Cu grid, some fresh Au NPs moved and attached to the former nanoseeds either by oriented attachment or by addition of Au atoms from reduction of Au^+ ions under the flowing and diffusion effect (as shown in step 2). Meanwhile, short Au nanorods were formed during this step. Due to the clean surfaces of the gold, oriented attachment (induced by direction of flow) could occur to form longer wires from short ones and single Au seeds during the following step (see Fig. S6, ESI†). Finally, under the constantly flow and diffuse of colloid solution, long Au NWs were successfully produced on the carbon membrane after been aged during the last step. In contrast, only short Au nanorods and Au particles were found on the horizontally placed Cu grid (see Fig. S7, ESI†). So the filter papers tilted 30° from the horizontal plane certainly enhanced the directional diffusion of seed solution, which may induce the formation of Au nanowires. These results indicate that the directional flow of solution and subsequent concentration/oriented attachment of nanoseeds on the tilted grid are the key factors for the organic-free synthesis of ultrathin gold

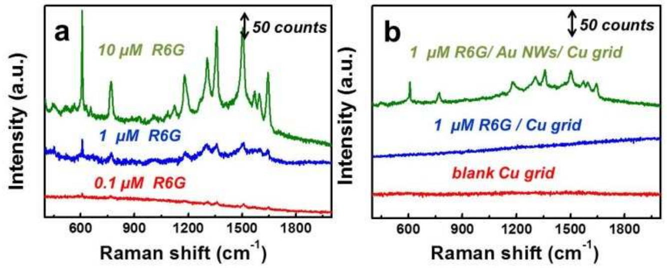

Fig. 5 (a) SERS spectra recorded for 10 µM (green line); 1 µM (blue line); 0.1 µM (red line) R6G on Cu grid supported Au NWs; (b) SERS spectra recorded for same R6G (1 µM) on different substrates, R6G on Cu grid supported Au NWs (green line); R6G on Cu grid (blue line), blank Cu grid (red line).

nanowires. Based on this mechanism, the growth of ultrathin Au NWs may be extended to some other substrates (*e.g.* glass, silicon wafer). Extending the synthesis on other flat substrates is now on the way.

This natural system of uniform Au NWs on carbon-coated Cu grid is an ideal substrate for SERS enhancement. In this sense, we compared its SERS abilities with blank substrates using Rhodamine 6G (R6G) which was widely used as probe molecule.[26-27] As shown in Fig. 5, Raman peaks observed at 609, 770, 1180, 1309, 1358, 1507, 1572, and 1645 cm^{-1} were consistent with the reported Raman signals of R6G calculated by Schatz *et al*.[28] The assignments of vibrations are listed in Table S1. Using data of SERS experiments, the detection limits could be as low as 1×10^{-7} M (see Fig. S8, ESI†). The analytical enhancement factor (AEF) is calculated followed the method used by Chiu,[29] which defined by the equation AEF = $(I_{SERS}/C_{SERS})/(I_{RS}/C_{RS})$. Here, I_{SERS} is the SERS intensity of R6G on the Au NWs; C_{SERS} is the concentration of R6G; while I_{RS} stands for the Raman intensity of R6G on a non-SERS active glass substrate (slide). Based on above experimental data, the AEF value of Au NWs located on Cu grid is 4.9×10^3. The details of calculations can be seen in the Supporting Information.

In summary, ultrathin Au NWs with an average diameter of 1.8 nm were *in situ* synthesized through a simple and efficient method on carbon-coated Cu grid. Ultrathin Au NWs were, for the first time, fabricated without using any template or organic reagent during the whole process. The flow of seed solution and subsequent concentration/oriented attachment of nanoseeds on the tilted grid may contribute to the formation of ultrathin Au NWs in absence of organic reagent. Furthermore, the substrate of Cu grid supported Au NWs was an ideal substrate for SERS measurement. The ultrathin nanowires obtained in this work hold great potential for both fundamental studies and more actual applications.

This work was financially supported by the National Basic Research Program (2009CB623504), the National Science Foundation of China (21173119, 21273109, 21303083), the Natural Science Foundation of Jiangsu Province (BK20130563) and the Fundamental Research Funds for the Central Universities.

Notes and references

*[a] *Key Laboratory of Mesoscopic Chemistry of MOE, School of Chemistry and Chemical Engineering, Nanjing University, Nanjing 210093, China*
E-mail: guoxf@nju.edu.cn.
[b] *Institute of Materials Research & Engineering, A*STAR (Agency for Science, Technology and Research), 3 Research Link, Singapore 117602, Singapore.*

† Electronic Supplementary Information (ESI) available: more details of synthesis and characterizations including TEM, as well as AEF calculations. See DOI: 10.1039/b000000x/

‡ Footnotes should appear here. These might include comments relevant to but not central to the matter under discussion, limited experimental and spectral data, and crystallographic data.

1 Y. N. Xia, P. D. Yang, Y. Sun, Y. Y. Wu, B. Mayers, B. Gates, Y. D. Yin, F. Kim and H. Q. Yan, *Adv. Mater.*, 2003, **15**, 353.
2. C. J. Murphy, A. M. Gole, S. E. Hunyadi and C. J. Orendorff, *Inorg. Chem.*, 2006, **45**, 7544.
3 R. Takahata, S. Yamazoe, K. Koyasu and T. Tsukuda, *J. Am. Chem. Soc.*, 2014, **136**, 8489.
4. A. Sánchez-Iglesias, B. Rivas-Murias, M. Grzelczak, J. Pérez-Juste, L. M. Liz-Marzán, F. Rivadulla and M. A. Correa-Duarte, *Nano Lett.*, 2012, **12**, 6066.
5. X. Hong, C. L. Tan, J. Z. Chen, Z. C. Xu and H. Zhang, *Nano Res.*, 2014, **8**, 40.
6. Y. L. Chen, C. Y. Lee and H. T. Chiu, *J. Mater. Chem. B.*, 2013, **1**,186.
7. C. H. Moon, M. Zhang, N. V. Myung and E. D. Haberer, *Nanotechnology*, 2014, **25**, 1.
8. W. L. Zhu, Y. J. Zhang, H. Y. Zhang, H. F. Lv, Q. Li, R. Michalsky, A. A. Peterson and S. H. Sun, *J. Am. Chem. Soc.*, 2014, **136**, 16132.
9. J. P. Xu and W. Jiang, *Macromolecules*, 2014, **47**, 2396.
10. Y. Chen, Z. Ouyang, M. Gu and W. L. Cheng, *Adv. Mater.*, 2013, **25**, 80.
11. X. Hong, D. S. Wang, and Y. D. Li, *Chem. Commun.*, 2011, **47**, 9909.
12. H. J. Feng, Y. M. Yang, Y. M. You, G. P. Li, J. Guo, T. Yu, Z. X. Shen, T. Wu and B. G. Xing, *Chem. Commun.*, 2009, **15**, 1984.
13. A. Halder and N. Ravishankar, *Adv. Mater.*, 2007, **19**, 1854.
14. X. M. Lu, M. S. Yavuz, H.-Y. Tuan, B. A. Korgel and Y. N. Xia, *J. Am. Chem. Soc.*, 2008, **130**, 8900.
15 Z. Y. Huo, C.-K. Tsung, W. Y. Huang, X. F. Zhang and P. D. Yang, *Nano Lett.*, 2008, **8**, 2041.
16 X. Huang, S. Z. Li, S. X. Wu, Y. Z. Huang, F. Boey, C. L. Gan and H. Zhang, *Adv. Mater.*, 2012, **24**, 979.
17. P. Kundu, U. Chandni, A. Ghosh and N. Ravishankar, *Nanoscale*, 2012, **4**, 433.
18. H. Liu, X. M. Cao, J. M. Yang, X. Q. Gong and X. Y. Shi, *Sci. Rep.* 2013, **3**, 3181.
19. Y. Imura, H. Tanuma, H. Sugimoto, R. Ito, S. Hojo, H. Endo, C. Morita and T. Kawai, *Chem. Commun.*, 2011, **47**, 6380.
20. Y. Imura, S. Hojo, C. Morita and T. Kawai, *Langmuir*, 2014, **30**, 1888.
21. H. Z. Cui, C. L. Hong, A. Ying, X. M. Yang and S. Q. Ren, *ACS Nano*, 2013, **7**, 7805.
22. A. Loubat, L. Impéror-Clerc, B. Pansu, F. Meneau, B. Raquet, G. Viau and L. Lacroix, *Langmuir*, 2014, **30**, 4005.
23. A. Loubat, L.-M. Lacroix, A. Robert, M. Impéror-Clerc, R. Poteau, L. Maron, R. Arenal, B. Pansu and G. Viau, *J. Phys. Chem. C.*, 2015, **119**, 4422.
24. B. Volosskiy, K. Niwa, Y. Chen, Z. P. Zhao, N. O. Weiss, X. Zhong, M. N. Ding, C. Lee, Y. Huang and X. F. Duan. *ACS Nano*, 2015, **9**, 3044.
25. M. Lin, L. Tng, T. Lim, M. Choo, J. Zhang, H. R. Tan, S. Q. Bai, *J. Phys. Chem.C.*, 2014, **118**, 10903.
26. Z. Y. Bao, J. Y. Dai, D. Y. Lei and Y. C. Wu, *J. Appl. Phys.*, 2013, **114**, 124305.
27. X. Y. Zhang, Y. H. Zheng, X. Liu, W. Lu, J. Y. Dai, D. Y. Lei and D. R. MacFarlane, *Adv. Mater.*, 2015, **27**, 1090.
28. L. Jensen and G. C. Schatz, *J. Phys. Chem. A.*, 2006, **110**, 5973.
29. Y. C. Yang, T. K. Huang, Y. L. Chen, J. Y. Mevellec, S. Lefrant, C. Y. Lee and H. T. Chiu, *J. Phys. Chem. C.*, 2011, **115**, 1932.